



HAL
open science

Reactive oxygen and iron species monitoring to investigate the electro-Fenton performances. Impact of the electrochemical process on the biodegradability of metronidazole and its by-products

A. Abou Dalle, F. Fourcade, A.A. Assadi, L. Domergue, Hayet Djelal, T. Lendormi, S. Taha, A. Amrane

► To cite this version:

A. Abou Dalle, F. Fourcade, A.A. Assadi, L. Domergue, Hayet Djelal, et al.. Reactive oxygen and iron species monitoring to investigate the electro-Fenton performances. Impact of the electrochemical process on the biodegradability of metronidazole and its by-products. *Chemosphere*, 2018, 199, pp.486-494. 10.1016/j.chemosphere.2018.02.075 . hal-01740153

HAL Id: hal-01740153

<https://univ-rennes.hal.science/hal-01740153>

Submitted on 4 May 2018

HAL is a multi-disciplinary open access archive for the deposit and dissemination of scientific research documents, whether they are published or not. The documents may come from teaching and research institutions in France or abroad, or from public or private research centers.

L'archive ouverte pluridisciplinaire **HAL**, est destinée au dépôt et à la diffusion de documents scientifiques de niveau recherche, publiés ou non, émanant des établissements d'enseignement et de recherche français ou étrangers, des laboratoires publics ou privés.

1 **Reactive oxygen and iron species monitoring to investigate the electro-**
2 **Fenton performances. Impact of the electrochemical process on the**
3 **biodegradability of metronidazole and its by-products.**

4 **Arwa ABOUDALLE^{a,b}, Florence FOURCADE^{a*}, Aymen Amin ASSADI^a, Lionel DOMERGUE^a,**
5 **Hayet DJELAL^{a,d}, Thomas LENDORMI^e, Samir TAHA^{b,c}, Abdeltif AMRANE^a**

6 *a. Univ rennes, Ecole Nationale Supérieure de Chimie de Rennes, CNRS, ISCR – UMR6226, F-35000 rennes, France*

7 *b. Laboratoire de Biotechnologies Appliquées, Centre AZM pour la recherche en biotechnologies et ses applications,*
8 *Ecole doctorale des sciences et technologies, Université Libanaise, Rue Al-Mitein, Tripoli, Liban.*

9 *c. Faculté de Santé Publique, Université Libanaise, quartier Dam et Farz, Tripoli, Liban.*

10 *d. Ecole des Métiers de l'Environnement, Campus de Ker Lann, 35170 Bruz, France*

11 *e. Université Bretagne Sud, FRE CNRS 3744, IRDL, F-56300 Pontivy, France*

12
13 **Abstract**

14 In this study, the monitoring of reactive oxygen species and the regeneration of the ferrous
15 ions catalyst were performed during electro-Fenton (EF) process to highlight the influence of
16 operating parameters. The removal of metronidazole (MTZ) was implemented in an
17 electrochemical mono-compartment batch reactor under various ranges of current densities,
18 initial MTZ and ferrous ions concentrations, and pH values. It was found that under 0.07 mA
19 cm⁻², 0.1 mM of ferrous ions and pH=3, the efficiency of 100 mg L⁻¹ MTZ degradation and
20 mineralization were 100 % within 20 min and 40% within 135 min of electrolysis,
21 respectively. The highest hydrogen peroxide and hydroxyl radical concentrations, 1.4 mM and
22 2.28 mM respectively, were obtained at 60 min electrolysis at 0.07 mA cm⁻². Improvement of
23 the biodegradability was reached from 60 min of electrolysis with a BOD₅/COD ratio above
24 0.4, which was reinforced by a respirometric study, that supports the feasibility of coupling
25 electro-Fenton and biological treatment for the metronidazole removal.

26

27 **Keywords:** Electro-Fenton process; Metronidazole; reactive oxygen species; ferrous ions
28 regeneration; respirometry; biodegradability

29

30 **1. Introduction**

31 Metronidazole (MTZ, 2-methyl-5-nitroimidazole-1-ethanol) is a nitroimidazole antibiotic, that
32 presents antibacterial and anti-inflammatory properties. MTZ is extensively used in Europe
33 for the treatment of infectious diseases caused by a wide range of anaerobic bacteria and
34 various protozoans, such as *Trichomonas vaginalis* and *Giardia lamblia* (Tally and Sullivan,
35 1981; Lau et al., 1992).

36 Because of its refractory character and a high solubility in water, MTZ is difficult to remove
37 during conventional sewage treatment (Kümmerer, 2001). Biorecalcitrance of this compound
38 was also demonstrated during culture of *Trametes Versicolor* fungus or using enzyme extract
39 from this fungus (Becker et al., 2016). As a result, MTZ accumulates in animals' body, fish-
40 farm waters and, more importantly, effluents from meat industries and hospitals (Kümmerer,
41 2001). Residual concentrations have consequently been detected in hospital effluents,
42 wastewater, surface water and groundwater (Dantas et al., 2010; Vulliet and Cren-Olivé,
43 2011). The results spotted that untreated release of MTZ exposes humans' health at risk
44 because of its potentially carcinogenic and mutagenic properties (Bendesky et al., 2002), its
45 toxicity against aquatic organisms (Lanzky and Halting-Sørensen, 1997) and genotoxicity to
46 humans since it causes a DNA damage in human lymphocytes (Ré et al., 1997).

47 Physico-chemical processes such as adsorption or ozonation can be performed to remove
48 refractory pharmaceutical pollutants in aqueous effluent including MTZ. Indeed, in their study
49 on MTZ adsorption, Rivera-Utrilla et al tested three different activated carbons. Results
50 showed the high adsorption capacity of the different activated carbons. Adsorption
51 phenomenon was more influenced by the activated carbons chemical properties rather than
52 their structural properties. Moreover, pH and the electrolyte concentration had a little

53 influence in the adsorption process, indicating a minor role of the electrostatic interactions
54 between MTZ and the activated carbons (Rivera-Utrilla et al., 2009). Adsorption is an
55 efficient process for MTZ removal but not destructive and then needs further post-treatment to
56 eliminate completely the pollutant.

57 Sánchez-Polo et al studied the removal of four different nitroimidazoles by ozonation process.
58 Low reactivity of nitroimidazoles with ozone was obtained with specific rate constants below
59 $350 \text{ M}^{-1} \text{ s}^{-1}$ and only 10-20% of organic carbon reduction (Sánchez-Polo et al., 2008).

60 Among physico-chemical processes, Advanced Oxidation Processes (AOPs) are considered as
61 promising technologies for water remediation, based on the *in-situ* generation of strong
62 oxidants such as hydroxyl radical that react non-selectively with most persistent organic
63 pollutants in aqueous solutions until they reach total mineralization (conversion into CO_2 ,
64 water and inorganic ions) (Latimer, 1952; Ku et al., 1999; Stasinakis, 2008; Brillas et al.,
65 2009).

66 Several AOPs were tested by Shemer and his co-workers (Shemer et al., 2006). They found
67 that the degradation of metronidazole by photolysis was low; the concentration decrease was
68 around 10% over a period of 5 min. The addition of H_2O_2 to the UV irradiation improved the
69 efficiency of the degradation and the best degradation yield reached 67% for the same
70 duration. On other way, during Fenton's process, the metronidazole degradation yield i.e the
71 concentration decrease was enhanced to 76% (Shemer et al., 2006). This process is well
72 known as one of the most efficient AOPs (Lopez et al., 2004). Its implementation and
73 maintenance are simple since that needs only hydrogen peroxide and ferrous ions (Eq. 1)
74 (Lopez et al., 2004; Lu et al., 2005; Pignatello et al., 2006). It had been widely applied for the
75 treatment and pre-treatment of wastewater (Trujillo et al., 2006).



77 When UV irradiation was applied in addition to the Fenton's reaction, quasi-total
78 metronidazole degradation was obtained (over 90%)(Shemer et al., 2006). Solar photo-Fenton
79 (Ammar et al., 2016) was also studied for the removal of metronidazole and based on COD
80 degradation, oxidation yield reached 96%.

81 Some studies based on the electro-Fenton process were carried out for the degradation of
82 metronidazole (Cheng et al., 2013; Pérez et al., 2015). This process is a combination of the
83 classical Fenton treatment with electrochemical reactions. It is based on the *in-situ* generation
84 of H₂O₂, brought by the continuous electrochemical reduction of dissolved oxygen as shown
85 in Eq. 2. Hydrogen peroxide reacts then with ferrous ions in catalytic amount to produce
86 hydroxyl radicals (Eq. 1) and ferrous ions were regenerated by their reduction at the cathode
87 surface. (Eq. 3) (Brillas et al., 2009).



90 Mineralization yield obtained with electro-Fenton did not exceed 40% in each study, and
91 increased to 53% with additional solar irradiation (Pérez et al., 2015).

92 For process intensification purpose in terms of mineralization, an alternative for the MTZ
93 removal was proposed. It concerned the improvement of biodegradability by the electro-
94 Fenton process prior to a subsequent biological mineralization (Mansour et al., 2012; Ferrag-
95 Siagh et al., 2014; Annabi et al., 2016; Olvera-Vargas et al., 2016; Ganzenko et al., 2017).

96 The interest of coupling physico-chemical process and biodegradation was already
97 highlighted (Scott and Ollis, 1995). In their study, the authors explained that the processes
98 order depends on the nature of the effluent to be treated. In presence of wastewater
99 concentrated in biorecalcitrant compounds, a chemical oxidation is required in order to
100 produce biodegradable by-products that will be then metabolized during the biological
101 process. Two sequences for the combination between electro-Fenton and biodegradation were

102 discussed for the removal of both 5-fluorouracil and caffeine at 0.1 mM (Ganzenko et al.,
103 2017). Both sequences were efficient for the removal of organic compounds. Biological pre-
104 treatment performances in a SBR reactor depended on microbial acclimation time and
105 biomass concentration. Residual organic load was then removed by electro-Fenton but a part
106 of the produced hydroxyl radicals was lost due to their attack on microorganism. During the
107 pre-pretreatment, pollutant biosorption could occur (Fontmorin et al., 2013) but was not
108 considered in this study. Moreover, the concentration of pollutants has an influence on the
109 biological treatment since for concentrations higher than their inhibitory threshold for
110 microorganisms; biodegradation could be less efficient (Yahiat et al., 2011). When electro-
111 Fenton was performed as pre-treatment, biodegradability was improved by increasing the
112 electrolysis time and the current intensity. However, regarding the economic feasibility of the
113 electrochemical pre-treatment, long electrolysis duration with a low current intensity was a
114 better option.

115 An increase of the BOD₅/COD ratio was obtained after the MTZ electro-Fenton treatment
116 (Cheng et al., 2013), but below the limit of biodegradability (Alonso Salles et al., 2010).

117 In this study, in order to reach the limit of biodegradability, the influence of some operating
118 parameters was considered in regard to the production and the monitoring of reactive oxygen
119 species (hydrogen peroxide, hydroxyl radicals) and in regard to the behavior of iron species in
120 solution during electrolysis. The electrochemical behavior of metronidazole was also
121 examined in order to understand its role in the compound degradation and mineralization.
122 Moreover, the estimation of biodegradability by means of the BOD₅/COD ratio was
123 supported by a respirometric study implemented during 21 d.

124

125 **2. Materials and methods**

126 **2.1. Chemicals and materials**

127 MTZ (2-methyl-5-nitroimidazole-1-ethanol) with 99% of purity was purchased from Sigma-
128 Aldrich (Saint-Quentin Fallavier, France). $\text{FeSO}_4 \cdot 7\text{H}_2\text{O}$ (purity 99%) and Na_2SO_4 (purity
129 99%) were used as a catalyst source and inert supporting electrolyte respectively, and were
130 obtained from Acros Organics (Thermo Fisher Scientific, Geel, Belgium). Acetonitrile (purity
131 99.9%) (HPLC grade) was also obtained from Sigma–Aldrich. All solutions were prepared
132 with ultrapure water and all other chemicals used for analysis were purchased from Acros and
133 Sigma.

134 2.2. Electrochemical Apparatus and Procedures

135 Experiments were performed at ambient temperature (20°C) in a discontinuous reactor
136 containing 250 mL of solution and were previously detailed (Abou Dalle et al., 2017). An
137 ammeter power supply (Microsonic systems, Microlab MX 20V-2A, France) delivered
138 cathodic current intensity throughout the electrolysis between two electrodes. A tri-
139 dimensional piece of graphite felt of 42 cm³ geometrical volume was used as cathode (Le
140 Carbone Lorraine RVG 4000 Mersen, Paris la Défense, France) and the anode was a platinum
141 cylinder (32 cm²). Compressed air was bubbled into the solution for 10 min before the
142 electrolysis to saturate the solution with O₂ and then throughout the experiments.
143 $\text{FeSO}_4 \cdot 7\text{H}_2\text{O}$ was added into the cell just before the beginning of the electrolysis. 50 mM
144 Na_2SO_4 was added as supporting electrolyte.

145

146 2.3 Analytical procedure

147 2.3.1. Electrochemical analysis

148 Current-potential curves were performed in a conventional three electrodes electrochemical
149 cell as previously detailed (Fourcade et al., 2013). The electrochemical apparatus was a
150 SP150 BioLogic potentiostat/galvanostat (BioLogic SAS, Clais, France) with EC-Lab[®]
151 software.

152 2.3.2. High Performance Liquid Chromatography (HPLC).

153 The degradation of Metronidazole was measured by HPLC using Waters 996 system
154 equipped with Waters 996 PDA (Photodiode Array Detector) and Waters 600LCD Pump. The
155 separation was achieved on Waters C 18 (5 μm ; 4.6×250 mm) reversed-phase. The eluent
156 consisted of an acetonitrile/water mixture (20/80, v/v) with 0.1% formic acid delivered at a
157 flow rate of 1 mL min^{-1} . The detection of Metronidazole was carried out at 318 nm and the
158 retention time was 4.3 min.

159 2.3.3. Total organic carbon (TOC) measurement.

160 TOC was measured by TOC- $V_{\text{CPH/CPG}}$ Total Organic Analyzer Shimadzu. CO_2 produced
161 from the combustion and the conversion of Organic Carbon compounds was identified by
162 non-dispersive Infra-Red Detector (NDIR).

163 2.3.4. Hydrogen peroxide quantification.

164 Hydrogen peroxide concentration was iodometrically measured with sodium thiosulfate as
165 titrant, by amperometric titration with a double Pt indicator electrode and an applied potential
166 difference of 100 mV (Potentio-amperometric TPA4 titrator, Tacussel, Lyon, France) (Abou
167 Dalle et al., 2017).

168 2.3.5. Hydroxyl radical's quantification

169 Dimethyl sulfoxide (DMSO) was used to trap hydroxyl radicals (Abou Dalle et al., 2017). It
170 reacts quickly with a hydroxyl radical forming methanesulfonic acid and sulfate (Jahnke,
171 1999). DIONEX DX120 ion chromatography was used to detect the formed methanesulfonic
172 acid. A DIONEX DX120 chromatograph was provided with a conductivity detector; the
173 stationary phase is constituted by an anion exchange column AS19 (4 x 250 mm) and the
174 mobile phase was constituted of a KOH solution in water. A gradient elution mode was
175 adopted for the analyses. 10 mM of KOH was considered during the first 10 min; then the
176 amount increased linearly to reach 45 mM from 10 to 25 min; and finally an amount of 45

177 mM of KOH was maintained from 25 to 35 min of the analysis. The flow rate remained
178 constant at 1 mL min⁻¹.

179 **2.3.6. Iron species quantification.**

180 Total dissolved iron species were quantified by atomic absorption spectrometry (AA140,
181 VARIAN spectrometer, Palo Alto, USA) with air/acetylene flame at 372 nm. Ferrous ions
182 were quantified by the orthophenanthroline complexometric method, detailed in a previous
183 work (Ben Hammouda et al., 2016).

184 **2.3.7. Biochemical oxygen demand (BOD₅) measurements**

185 The inoculated activated sludge was obtained from a municipal wastewater treatment plant
186 (Beaurade, Rennes, France). The activated sludge was cultivated under oxygen flow on a
187 previously detailed mineral medium (Fontmorin et al., 2012). Before inoculation, the
188 activated sludge was washed three times with tap water and twice with ultrapure water to
189 remove all carbon residues. A verification of the elimination of these latter was carried out by
190 analyzing the TOC values.

191 BOD₅ measurements were carried out in Oxitop IS6 (WTW, Alès, France) under a previously
192 detailed protocol (Fontmorin et al., 2012).

193 **2.3.8. Respirometric experiments**

194 Experiments were carried out in 3L bioreactor (Bioflow 3000, New Brunswick scientific)
195 coupled to a respirometric device measuring Oxygen Uptake Rates (OUR) of activated sludge
196 (Spérandio and Paul, 2000; Adouani et al., 2015). This latter was collected from the biological
197 basin of Pontivy (Brittany, France) Waste Water Treatment Plant.

198 2.5 L of settled sludge, after sifting at 400 µm, were aerated in the bioreactor; pH and
199 temperature were controlled to 7.7 and 25°C respectively. Dissolved oxygen uptake rate was
200 measured continuously in the bioreactor. Biological activity of heterotrophic biomass can be
201 then characterized as well as its behavior (a possible microorganism's inhibition for example)

202 in the presence of 500 mg L⁻¹ MTZ or its electrolyzed solutions. First, endogenous respiration
203 was measured (OUR_{endo}). To characterize heterotrophic biomass activity, a biodegradable
204 carbon source, here sodium acetate (0.1 g), was firstly added in the culture medium when
205 OUR_{endo} was stable and exogenous respiration (OUR)_{exo} was measured. MTZ or electrolyzed
206 solution was then added to reach TOC values in the range 5-50 mg C L⁻¹ in the bioreactor.
207 When the OUR_{endo} remained stable, sodium acetate was added again, the response of OUR_{exo}
208 was compared with the previous one. To characterize autotrophic biomass activity, sodium
209 acetate was replaced by a mineral substrate (NH₄Cl 0.1 g). These tests were performed during
210 21 d. The analysis of the different curve patterns (OUR function of time) provided
211 information on the metabolization of each substrate.

212

213 3. Results and discussion

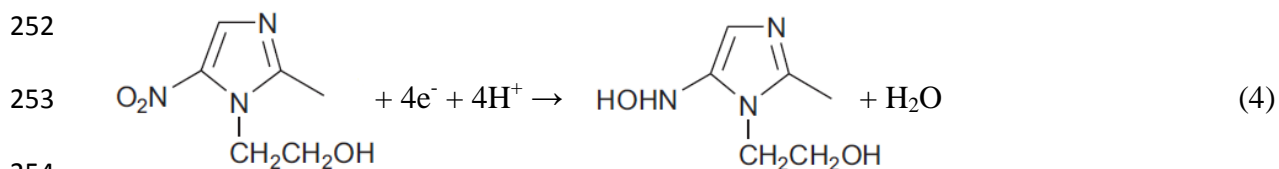
214 3.1. Evolution of MTZ degradation and mineralization

215 Metronidazole degradation and mineralization were first studied during electrolysis at 0.04
216 mA cm⁻² in a 50 mM sodium sulfate solution at pH 3 with 0.1 mM of ferrous ions and for an
217 initial concentration of 100 mg L⁻¹. The degradation kinetic was rapid compared to the
218 mineralization kinetic since an almost total degradation of the target compound was obtained
219 at 25 min. After 135 min of electrolysis, mineralization yield was only 26% (Fig 1a). The
220 recalcitrance of metronidazole by-products during electro-Fenton treatment was already
221 noticed by Pérez et al. (Pérez et al., 2015) and could explain the moderate mineralization yield
222 obtained. In their study, the identified heterocyclic by-products included an imidazole ring
223 that is considered as stable because of the presence of two nitrogen atoms in the aromatic
224 cycle. In the imidazole ring, a free electron doublet associated to the pyrrole nitrogen is
225 delocalized in the cycle and electrons from pyridine nitrogen are localized in its sp² orbital.
226 This particular configuration confers stability to the imidazole ring (Clayden et al., 2002) and

227 could then confer its recalcitrance toward hydroxyl radical attack. In the same way, cyanuric
228 acide is well known as recalcitrant to hydroxyl radical oxidation due to the electron deficiency
229 of the triazine ring linked to the higher electronegativity of nitrogen compared to that of
230 carbon (Liu, 2014).

231 Different evolutions for MTZ concentration during electrolysis conducted at 0.07 mA cm^{-2}
232 with 0.1 mM of ferrous ions were plotted according to the initial target compound
233 concentration in the range of $100\text{-}500 \text{ mg L}^{-1}$ (Fig. SM-1). As almost total degradation was
234 obtained after 20 min for 100 mg L^{-1} MTZ initial concentration, the time needed for a total
235 degradation increased to 30 min doubling the initial concentration. If we considered a pseudo
236 first order kinetic for the global degradation as mentioned in most of the studies on the
237 electro-Fenton process (Brillas et al., 2009), apparent initial kinetic constant (k_{app}) deduced
238 from the 10 first min of electrolysis (Table 1) highlighted a higher reaction kinetic for an
239 initial concentration of 100 mg L^{-1} . Then k_{app} decreased with the initial MTZ concentration.
240 These results were in accordance with previous studies (Ferrag-Siagh et al., 2014; Annabi et
241 al., 2016) and can be explained by a gradual acceleration of competitive reactions between the
242 degradation of the target compound and that of its by-products.

243 The electrochemical behavior of metronidazole was also studied in order to study the
244 contribution of a direct oxidation and/or reduction of the target molecule at the electrode
245 surface during the electro-Fenton process. For this purpose, current potential curves were
246 plotted with a vitreous carbon rotating disk electrode in Na_2SO_4 50 mM supporting electrolyte
247 at pH 3 with 100 mg L^{-1} of the target compound and under nitrogen atmosphere. No MTZ
248 oxidation was highlighted (data not show) while a signal for MTZ reduction was observed
249 around -0.4 V/SCE (Fig. 1b). The MTZ electrochemical reaction was already highlighted by
250 Saïdi et al. (Saïdi et al., 2014) in acidic aqueous medium H_2SO_4 (0.5 M) and corresponded to
251 the four-electrons reduction of the nitro group to the corresponding hydroxylamine (Eq. 4).



255 During MTZ electrolysis in the same operating conditions as for electro-Fenton but in the
 256 presence of tert-butanol, well-known as an hydroxyl radical's scavenger (Ma and Graham,
 257 2000), kinetic of MTZ degradation was slower since an almost total degradation was obtained
 258 for around 40 min (not shown) compared to 25 min for electrolysis without tert-butanol. The
 259 electric charge (Q) was calculated using the Faraday's law (Eq. 5) with F the Faraday
 260 constant, N the mol number of degraded MTZ and n the 4 electrons reduction of
 261 metronidazole. According to the consumed electric charge during 40 min of electrolysis in the
 262 presence of tert-butanol (Eq. 6), the current efficiency was about 47%.

263
$$Q = n F N \quad (5)$$

264
$$Q = i t \quad (6)$$

265 It can be therefore supposed that metronidazole degradation was due to both the
 266 electrochemical reduction at the cathode surface and the oxidation by hydroxyl radicals.
 267 Under nitrogen atmosphere to avoid the presence of oxygen in the solution and then the
 268 production of hydrogen peroxide, mineralization yield was negligible (not shown). This result
 269 confirms that metronidazole mineralization was mainly due to the action of hydroxyl radicals
 270 produced by the Fenton reaction.

271

272 **3.2. Effect of the applied cathodic current density**

273 **3.2.1. Effect of the applied cathodic current density on MTZ degradation and mineralization**

274 Current density is one of the main parameters governing the efficiency of the electro-Fenton
 275 process, governing the formation of H₂O₂ and then that of hydroxyl radicals (Oturán et al.,
 276 2008; Özcan et al., 2009; Feng et al., 2014). Cathodic current density affects the organic

277 matter treatment performance (Brillas et al., 2000). Its impact on the degradation and the
278 mineralization of MTZ was therefore examined. The figure 2a shows the evolution of
279 metronidazole concentration as a function of time for different cathodic current densities
280 ranging from 0.04 to 0.45 mA cm⁻². The obtained results showed an almost total degradation
281 except for 0.04 mA cm⁻² after 15 min of electrolysis (Fig. 2a). In the range 0.07 to 0.22 mA
282 cm⁻², the k_{app} were nearly similar, in a short range of values, 0.22 to 0.24 min⁻¹ (Table 1),
283 while for 0.04 mA cm⁻², the apparent constant kinetics was low, about 0.08 min⁻¹. The weak
284 maximum value observed for 0.07 mA cm⁻² should however be noticed.

285 This faster oxidation at 0.07 mA cm⁻² can be ascribed to an acceleration of the H₂O₂
286 formation rate according to reaction (Eq. 2) and was confirmed by the hydrogen peroxide
287 quantification (Fig. 3b). A good regeneration of ferrous ions from reaction (Eq. 3), as
288 mentioned in paragraph 3.2.2., can also explain the better efficiency of the electro-Fenton
289 process at 0.07 mA cm⁻² if compared to higher current densities (Brillas et al., 2009). At
290 higher current densities, the production of hydrogen peroxide was lower (Fig. 3b).

291 As observed in Fig. 3a, plotting the concentration decrease according to the electric charge
292 (Q) highlighted the presence of competitive reactions since the necessary electric charge for a
293 total degradation increased with the current density. At 0.07 mA cm⁻², total degradation was
294 obtained for an electric charge of 120 C. When current density increased to 0.45 mA cm⁻²
295 total MTZ degradation required more than 600 C. Concurrent reactions such as the direct 4
296 electrons oxygen reduction (Eq. 7), hydrogen peroxide reduction (Eq. 8) or formation of
297 hydrogen (Eq. 9) at the cathode and the oxidation of H₂O₂ on the anode (Eq.10) in the
298 undivided cell can impede the accumulation of hydrogen peroxide (Brillas et al., 2009; Dirany
299 et al., 2012; Ferrag-Siagh et al., 2013). Because of these competing reactions, the constant
300 rate k_{app} (Table 1) cannot be proportional to the current density (Annabi et al., 2016).





305

306 Mineralization yields remained limited irrespective of the applied current density (Fig. 2b)
307 due to the recalcitrance of metronidazole by-products as mentioned before. For instance, for a
308 current density of 0.04 mA cm^{-2} , the TOC removal was only 26 % after 135 min of treatment.
309 TOC removal increased to 40 % with a current density of 0.07 mA cm^{-2} . This highest
310 mineralization yield was also in accordance with the highest concentration of hydrogen
311 peroxide obtained, 1.4 mM (Fig. 3b); while a lower production of hydrogen peroxide was
312 observed for a further increase of the current density.

313

314 **3.2.2. Effect of the current density on the concentration of iron species.**

315 The evolution of the ferrous and ferric ions concentrations in the solution during the electro-
316 Fenton process at different current densities is presented in Fig. 4a. The total concentration of
317 iron ions remained constant throughout the electrolysis for 0.04 mA cm^{-2} ; while a decrease of
318 this concentration of about 15% was observed when the current density increased to 0.07 mA
319 cm^{-2} . For 0.22 and 0.45 mA cm^{-2} , an almost total disappearance of the total iron ions in
320 solution was observed from 60 min of electrolysis. Indeed, for high current densities, water
321 reduction can lead to a local alkalization of the solution caused by hydroxyl anions
322 formation during H_2 release and then to the precipitation of iron as $\text{Fe}(\text{OH})_3$ (Eq. 11) (Brillas
323 et al., 2009; Petrucci et al., 2016).



325 The adsorption of iron hydroxide onto the electrode surface (Petrucci et al., 2016) or the
326 reduction of iron ions to metallic iron considering standard potentials for iron redox couples,
327 could be checked even if no deposit on the electrode surface was observed after electrolysis.
328 All these phenomena could then partly explain a lower efficiency for these current densities.
329 In order to study the regeneration of ferrous ions, electrolysis at 0.04 and 0.07 mA cm⁻² were
330 carried out under N₂ inert atmosphere, in order to avoid dissolved O₂ and then the electro-
331 generation of H₂O₂ (Fig. 4b). An initial amount of ferric ions of 0.1 mM was added into the
332 reactor at pH 3. At the initial time, without electrodes polarization, the slight amount of
333 ferrous ions detected can be explained by redox equilibrium between ferrous and ferric ions in
334 solution. Since the electrodes polarization, ferrous ions were detected very quickly in solution
335 at a value of 0.06 mM for both current densities, and remained then stable throughout
336 electrolysis. 60% of ferric ions were reduced at the cathode surface and as the concentration
337 of total iron ions in solution remained quasi constant in solution, 40% of ferric ions remained
338 in solution; this could be explained by an equilibrium between ferrous and ferric ions
339 implemented in solution throughout the electrolysis. In addition, the evolution of ferrous ions
340 generation was similar for both current intensities, as for the total concentration of iron
341 species. The difference observed between 0.04 and 0.07 mA cm⁻² concerning mineralization
342 can be then explained by the higher production of hydrogen peroxide measured for the latter
343 current density.

344

345 **3.3. Influence of the initial catalyst concentration**

346 In order to evaluate the effect of the catalyst concentration on the degradation and the
347 mineralization of Metronidazole, several experiments were performed in the presence of 100
348 mg L⁻¹ of MTZ at pH 3 and an applied current density of 0.07 mA cm⁻². The degradation of
349 the target compound was slightly influenced by the concentration of ferrous ions in the

350 studied range from 0.05 to 1 mM (Fig. SM-2). Indeed, for 15 min of electrolysis, degradation
351 yields were in a short range of values, 90 to 99% with a slight peak (99%) for 0.1 mM of
352 catalyst. Because of the electrochemical reduction of metronidazole at the cathode surface and
353 a good regeneration of ferrous ions at these current densities, the influence of the ferrous ions
354 amount on the metronidazole degradation can be considered as low in this range of
355 concentrations. MTZ mineralization also showed a slight peak in the range of catalyst
356 concentrations tested; it increased from 20% to 32% at 120 min of electrolysis for increasing
357 Fe^{2+} concentrations from 0.05 to 0.1 mM respectively (Fig. SM-2). This increase could be
358 attributed to the increase of the production of hydroxyl radicals from 1.52 to 2.28 mM
359 respectively (Table 2). The MTZ mineralization and the production of hydroxyl radicals
360 remained then constant for 0.5 mM and then decreased for 1 mM of ferrous ions. For this
361 latter ferrous concentration, mineralization yield was 23% after 120 min and the concentration
362 of produced hydroxyl radical decreased to 1.56 mM for 60 min of electrolysis respectively
363 (Fig. SM-2 and Table 2). This decrease can be explained by competition effects between
364 hydroxyl radicals resulting from the Fenton's reaction and the excess of ferrous ions (Panizza
365 and Cerisola, 2009), according to Eq. 12.



367 It can be therefore deduced that the optimal value for ferrous ions was 0.1 mM. This value
368 was in accordance with other studies, such as the mineralization by the electro-Fenton process
369 of tetracycline (Ferrag-Siagh et al., 2013) , direct orange 61 (Hammami et al., 2007) and
370 pentachlorophenol (Oturán et al., 2001). However, the influence of this parameter is not
371 essential in this range of concentrations since the difference between the mineralization yields
372 for all tested ferrous ions concentrations did not exceed 12%.

373

374

375 3.4. Effect of the pH

376 To consider the effect of pH on the electro-Fenton process, degradation and mineralization of
377 MTZ were studied at different pH values from 2 to 9. The degradation of metronidazole was
378 achieved by the Fenton's reaction and such reaction is highly related to the pH (Brillas et al.,
379 2009). Moreover, it was also shown that the electrochemical reduction of metronidazole
380 depends also on the pH (Saïdi et al., 2014), in agreement with the impact of the pH on the
381 degradation rate of metronidazole experimentally observed (Table 1). Indeed, for acidic
382 media, values of k_{app} (0.18 and 0.17 min^{-1} for pH 2 and 3 respectively) were higher compared
383 to those obtained in neutral and basic media (0.08, 0.08, 0.05 min^{-1} for pH 5, 7 and 9
384 respectively). The mineralization yields decreased from 32% to 24% after 120 min when pH
385 decreased from 3 to 2 respectively (Fig. SM-3). At higher pH values, the degradation of
386 metronidazole was very slow (Fig. SM-3) and reached 83.0%, 80.7%, 65.4% after 30 min,
387 while mineralization yields were 17.0%, 8.3%, and 5.9% after 2 hours for pH 5, pH 7 and pH
388 9 respectively. Optimal mineralization yield (32%) was obtained at pH 3. Higher amounts of
389 hydroxyl radicals were obtained at acidic pH (Table 2) and the optimal production of
390 hydroxyl radicals was reached at pH 3, that is consistent with the related literature (Qiang et
391 al., 2003; Ramirez et al., 2005; Zhou et al., 2007; Ramirez et al., 2009). At pH values lower
392 than 3, ferric ions can form complexes with hydrogen peroxide leading to lower production of
393 hydroxyl radicals (1.95 ± 0.09 mM – Table 2). Moreover, The H_2 evolution can be favored at
394 acidic pH (Petrucci et al., 2016) and hydrogen peroxide would form an oxonium ion (Eq. 13)
395 which inhibits the formation of hydroxyl radicals (Sun et al., 2009; Zhou et al., 2013). For
396 higher values of pH, the precipitation of ferric ions (Eq. 14) and then a lower production of
397 hydroxyl radicals (Table 2) leads to a loss of efficiency (Brillas et al., 2009; Masomboon et
398 al., 2009; Nidheesh and Gandhimathi, 2012).





401

402 **4. Biodegradability of the electrolyzed solution of MTZ**

403 Once the solution was treated by electro-Fenton, since organic carbon was still present in
404 solution due to low mineralization yield, a combined process involving a subsequent
405 biological treatment could be considered in order to complete the mineralization of the
406 electrolyzed solution. To assess the relevance of such combined process, the biodegradability
407 should be first determined, it corresponded to the BOD₅ on COD ratio; a solution is
408 considered as easily biodegradable from a ratio of 0.4 (Alonso Salles et al., 2010).

409 Table 3 reported the time-course of the ratio values of 100 mg L⁻¹ MTZ electrolysis at 0.07
410 mA cm⁻² and with 0.1 mM of ferrous ions. BOD₅ /COD ratio values suggested that the initial
411 MTZ solution was not biodegradable. After 30 min of electrolysis, even if a total degradation
412 of MTZ was observed (Fig. 1), the solution remained not biodegradable with a ratio of 0.24,
413 showing that the MTZ by-products, at this time of electrolysis, were relatively resistant to
414 micro-organisms since these components were structurally close to the target compound
415 (Mansour et al., 2012). However, the slight improvement of biodegradability can be due to
416 short linear aliphatic carboxylic acids resulting from the loss of lateral ethanol and acetic acid
417 group during the oxidation of MTZ and its heterocyclic intermediates (Pérez et al., 2015) that
418 can be metabolized by microorganisms. The solution became biodegradable since the ratio
419 value reached 0.7 for 120 min of electrolysis (Table 3). It can be therefore supposed that a
420 large part of recalcitrant by-products was oxidized beyond 60 min since the ratio reached 0.46
421 and can be therefore considered as an optimal oxidation time to minimize the energy
422 consumption. Respirometric experiments showed that no inhibition of heterotrophic and
423 autotrophic biomasses was observed whether after the injection of a non-electrolyzed solution
424 of MTZ or an electrolyzed one. Whereas no response in OUR curve was observed with a non-

425 electrolyzed solution of MTZ at the beginning of the test, direct response was observed with
426 the first injection of the electrolyzed solution of MTZ which supported the BOD₅ results (data
427 not show). Moreover, after 18 d, a response in OUR curve was observed with a non-
428 electrolyzed solution of MTZ (data not show), which would prove that biomass could be
429 acclimatized to MTZ and perform its direct degradation. The biodegradability improvement
430 after electro-Fenton treatment of recalcitrant compounds was also noticed in several reports
431 (Alonso Salles et al., 2010; Mansour et al., 2012; Ferrag-Siagh et al., 2014; Annabi et al.,
432 2016). Even if the respirometric study assumed a possible biodegradation of pure MTZ after
433 18 d, the electro-Fenton pretreatment should allow to significantly decrease the
434 biodegradation duration.

435 **4. Conclusion**

436 The degradation and mineralization of metronidazole was studied by the electro-Fenton
437 process in a mono-compartment discontinuous reactor including a carbon felt cathode and a
438 platinum anode. Both the MTZ electrochemical reduction at the cathode surface and the
439 Fenton reaction were responsible for the degradation of the target compound. However,
440 mineralization was mainly due to the production *in-situ* of hydroxyl radicals. The influence of
441 some operating parameters such as initial Metronidazole's concentration, current intensity,
442 initial Fe²⁺ concentration, and pH value was examined. The highest generation of hydrogen
443 peroxide was obtained at 0.07 mA cm⁻² with a good regeneration of ferrous ions and at this
444 current density, production of hydroxyl radicals was the highest at pH 3 with 0.1 mM ferrous
445 ions. These conditions were considered as optimal and allowed a total degradation of MTZ
446 and 40% mineralization within 20 min and 135 min of electrolysis, respectively. Additionally,
447 an improvement of the biodegradability to 0.46 was reached from 60 min of electrolysis and
448 was supported by respirometry, indicating the relevance of the electro-Fenton process as a
449 pretreatment prior to a subsequent biological treatment to complete the mineralization.

450

451 **References**

452 Abou Dalle, A., Domergue, L., Fourcade, F., Assadi, A.A., Djelal, H., Lendormi, T., Soutrel,
453 I., Taha, S., Amrane, A., 2017. Efficiency of DMSO as hydroxyl radical probe in an
454 Electrochemical Advanced Oxidation Process – Reactive oxygen species monitoring and
455 impact of the current density. *Electrochim. Acta* 246, 1-8.

456

457 Adouani, N., Limousy, L., Lendormi, T., Sires, O., 2015. N₂O and NO emissions during
458 wastewater denitrification step: Influence of temperature on the biological process. *C.R.
459 Chimie* 18, 15-22.

460

461 Alonso Salles, N., Fourcade, F., Geneste, F., Floner, D., Amrane, A., 2010. Relevance of an
462 electrochemical process prior to a biological treatment for the removal of an
463 organophosphorous pesticide, phosmet. *J. Hazard. Mater.* 181, 617-623.

464

465 Ammar, H.B., Ben Brahim, M., Abdelhédi, R., Samet, Y., 2016. Enhanced degradation of
466 metronidazole by sunlight via photo-Fenton process under gradual addition of hydrogen
467 peroxide. *J. Mol. Catal. A.-Chem.* 420, 222-227.

468

469 Annabi, C., Fourcade, F., Soutrel, I., Geneste, F., Floner, D., N., B., Amrane, A., 2016.
470 Degradation of enoxacin by the electro-Fenton process: optimization, biodegradability
471 improvement and degradation mechanism. *J. Environ. Manage.* 165, 96-105.

472

473 Becker, D., Della Giustina, S.V., Rodriguez-Mozaz, S., Schoevaart, R., Barceló, D., De
474 Cazes, M., Belleville, M.P., Sanchez-Marcano, J., De Gunzburg, J., Couillerot, O., Völker, J.,
475 Oehlmann, J., Wagner, M., 2016. Removal of antibiotics in wastewater by enzymatic
476 treatment with fungal laccase – Degradation of compounds does not always eliminate toxicity.
477 *Bioresource Technol.* 219, 500-509.

478

479 Ben Hammouda, S., Fourcade, F., Assadi, A., Soutrel, I., Adhoum, N., Monser, L., Amrane,
480 A., 2016. Effective heterogeneous electro-Fenton process for the degradation of a malodorous
481 compound, indole, using iron loaded alginate beads as a reusable catalyst. *Appl. Catal. B-
482 Environ.* 182, 47-58.

483

484 Bendesky, A., Menéndez, D., Ostrosky-Wegman, P., 2002. Is metronidazole carcinogenic?
485 *Mutat. Res- Rev. Mutat.* 511, 133-144.

486

487 Brillas, E., Calpe, J.C., Casado, J., 2000. Mineralization of 2,4-D by advanced
488 electrochemical oxidation processes. *Water Res.* 34, 2253-2262.

489

490 Brillas, E., Sirés, I., Oturan, M.A., 2009. Electro-Fenton process and related electrochemical
491 technologies based on Fenton's reaction chemistry. *Chem. Rev.* 109, 6570-6631.

492

493 Cheng, W., Yang, M., Xie, Y., Liang, B., Fang, Z., Tsang, E.P., 2013. Enhancement of
494 mineralization of metronidazole by the electro-Fenton process with a Ce/SnO₂-Sb coated
495 titanium anode. *Chem. Eng. J.* 220, 214-220.

496

- 497 Clayden, J., Greeves, N., Warren, S., Wothers, P., 2002. *Chimie Organique*. First ed. De
498 Boeck, Paris.
- 499 Dantas, R.F., Rossiter, O., Teixeira, A.K.R., Simões, A.S., Da Silva, V.L., 2010. Direct UV
500 photolysis of propranolol and metronidazole in aqueous solutions. *Chem. Eng. J.* 158, 143-
501 147.
- 502
- 503 Dirany, A., Sirés, I., Oturan, N., Özcan, A., Oturan, M.A., 2012. Electrochemical treatment of
504 the antibiotic sulfachloropyridazine: kinetics, reaction pathways and toxicity evolution.
505 *Environ. Sci. Technol.* 46, 4074-4082.
- 506
- 507 Feng, L., N., O., Van Hullebusch, E.D., Esposito, G., Oturan, M.A., 2014. Degradation of
508 anti-inflammatory drug ketoprofen by electro-oxidation: comparison of electro-Fenton and
509 anodic oxidation processes. *Environ. Sci. Pollut. R.* 21, 8406-8416.
- 510
- 511 Ferrag-Siagh, F., Fourcade, F., Soutrel, I., Aït-Amar, H., Djelal, H., Amrane, A., 2013.
512 Tetracycline degradation and mineralization by the coupling of an electro-Fenton
513 pretreatment and a biological process. *J. Chem. Technol. Biot.* 88, 1380-1386.
- 514
- 515 Ferrag-Siagh, F., Fourcade, F., Soutrel, I., Aït Amar, H., Djelal, H., Amrane, A., 2014.
516 Electro-Fenton pretreatment for the improvement of tylosin biodegradability. *Environ. Sci.*
517 *Pollut. R.* 21, 8534-8542.
- 518
- 519 Fontmorin, J.M., Fourcade, F., Geneste, F., Floner, D., Huguet, S., Amrane, A., 2013.
520 Combined process for 2,4-dichlorophenoxyacetic acid treatment - Coupling of an
521 electrochemical system with a biological treatment. *Biochem. Eng. J.* 70, 17-22.
- 522
- 523 Fontmorin, J.M., Huguet, S., Fourcade, F., Geneste, F., Floner, D., Amrane, A., 2012.
524 Electrochemical oxidation of 2,4-dichlorophenoxyacetic acid: analysis of by-products and
525 improvement of the biodegradability. *Chem. Eng. J.* 195-196, 208-217.
- 526
- 527 Fourcade, F., Delawarde, M., Guihard, L., Nicolas, S., Amrane, A., 2013. Electrochemical
528 reduction prior to electro-Fenton oxidation of azo dyes: Impact of the pretreatment on
529 biodegradability. *Water Air Soil Poll.* 224, 1-11.
- 530
- 531 Ganzenko, O., Trelu, C., Papirio, S., Oturan, N., Huguenot, D., Van Hullebusch, E.D.,
532 Esposito, G., Oturan, M.A., 2017. Bioelectro-Fenton: evaluation of a combined biological-
533 advanced oxidation treatment for pharmaceutical wastewater. *Envir. Sci. Pollut. R.* doi:
534 10.1007/s11356-017-8450-6.
- 535
- 536 Hammami, S., Oturan, N., Bellakhal, N., Dachraoui, M., Oturan, M.A., 2007. Oxidative
537 degradation of direct orange 61 by electro-Fenton process using a carbon felt electrode:
538 Application of the experimental design methodology. *J. Electroanal. Chem.* 610, 75-84.
- 539
- 540 Jahnke, L.S., 1999. Measurement of hydroxyl radical - generated methane sulfinic acid by
541 high-performance liquid chromatography and electrochemical detection. *Anal. Biochem.* 269,
542 273-277.
- 543
- 544 Ku, Y., Chen, K., Lee, K., 1999. Ultrasonic destruction of 2-chlorophenol in aqueous
545 solution. *Water Res.* 31, 929-935.
- 546

- 547 Kümmerer, K., 2001. Drugs in the environment: emission of drugs, diagnostic aids and
548 disinfectants into wastewater by hospital in relation to other sources - a review. *Chemosphere*
549 45, 957-969.
- 550
- 551 Lanzky, P.F., Halting-Sørensen, B., 1997. The toxic effect of the antibiotic metronidazole on
552 aquatic organisms. *Chemosphere* 35, 2553-2561.
- 553
- 554 Latimer, W.M., 1952. *Oxidation potentials*. Prentice Hall, New York.
- 555
- 556 Lau, A.H., Lam, N.P., Piscitelli, S.C., Wilkes, L., Danziger, L.H., 1992. Clinical
557 pharmacokinetics of metronidazole and other nitroimidazole anti-infectives. *Clin.*
558 *Pharmacokinet.* 23, 328-364.
- 559
- 560 Liu, G., 2014. Recalcitrance of cyanuric acid to oxidative degradation by OH radical:
561 theoretical investigation. *RSC Adv.* 4, 37359-37364.
- 562
- 563 Lopez, A., Pagano, M., Volpe, A., Di Pinto, A.C., 2004. Fenton's pre-treatment of mature
564 landfill leachate. *Chemosphere* 54, 1005-1010.
- 565
- 566 Lu, M.C., Zhang, H., Huang, Y.Y., Wang, S.Y., 2005. Influence of organic ions on the
567 mineralization of 2,4-dinitrophenol by the Fenton reaction. *Fresen. Environ. Bull.* 14, 101-
568 104.
- 569
- 570 Ma, J., Graham, N.J., 2000. Degradation of atrazine by manganese-catalyzed ozonation -
571 influence of radical scavenger. *Water Res.* 34, 3822-3828.
- 572
- 573 Mansour, D., Fourcade, F., Bellakhal, N., Dachraoui, M., Hauchard, D., Amrane, A., 2012.
574 Biodegradability improvement of sulfamethazine solutions by means of electro-Fenton
575 Process. *Water Air Soil Poll.* 223, 2023-2034.
- 576
- 577 Masomboon, N., Ratanatamskul, C., Lu, M.C., 2009. Chemical oxidation of 2,6-
578 dimethylaniline in the Fenton process. *Environ. Sci. Technol.* 43, 8629-8634.
- 579
- 580 Nidheesh, P.V., Gandhimathi, R., 2012. Trends in electro-Fenton process for water and
581 wastewater treatment: An overview. *Desalination* 299, 1-15.
- 582
- 583 Olvera-Vargas, H., Cocerva, T., Oturan, N., Buisson, D., Oturan, M.A., 2016. Bioelectro-
584 Fenton: A sustainable integrated process for removal of organic pollutants from water:
585 Application to mineralization of metoprolol. *J. Hazard. Mater.* 319, 13-23.
- 586
- 587 Oturan, M.A., Oturan, N., Lahitte, C., Trevin, S., 2001. Production of hydroxyl radicals by
588 electrochemically assisted Fenton's reagent: application to the mineralization of an organic
589 micropollutant, pentachlorophenol. *J. Electroanal. Chem.* 507, 96-102.
- 590
- 591 Oturan, M.A., Pimentel, M., Oturan, N., Sirés, I., 2008. Reaction sequence for the
592 mineralization of the short-chain carboxylic acids usually formed upon cleavage of aromatics
593 during electrochemical Fenton treatment. *Electrochim. Acta* 54, 173-182.
- 594
- 595 Özcan, A., Oturan, M.A., Oturan, N., Sahin, Y., 2009. Removal of Acid Orange 7 from water
596 by electrochemically generated Fenton's reagent. *J. Hazard. Mater.* 163, 1213-1220.

- 597
598 Panizza, M., Cerisola, G., 2009. Electro-Fenton degradation of synthetic dyes. *Water Res.* 43,
599 339-344.
600
- 601 Pérez, T., Garcia-Segura, S., El-Ghenymy, A., Nava, J.L., Brillas, E., 2015. Solar
602 photoelectro-Fenton degradation of the antibiotic metronidazole using a flow plant with a
603 Pt/air-diffusion cell and a CPC photoreactor. *Electrochim. Acta* 165, 173-181.
604
- 605 Petrucci, I., Da Pozzo, A., Di Palma, L., 2016. On the ability to electrogenerate hydrogen
606 peroxide and to regenerate ferrous ions of three selected carbon-based cathodes for electro-
607 Fenton processes. *Chem. Eng. J.* 283, 750-758.
608
- 609 Pignatello, J.J., Oliveros, E., Mac Kay, A., 2006. Advanced oxidation processes for organic
610 contaminant destruction based on the Fenton reaction and related chemistry. *Crit. Rev. Env.*
611 *Sci. Tec.* 36, 1-84.
612
- 613 Qiang, Z., Chang, J.H., Huang, C.P., 2003. Electrochemical generation of Fe^{2+} in Fenton
614 oxidation processes. *Water Res.* 37, 1308-1319.
615
- 616 Ramirez, H.J., Costa, C.A., Madeira, L.M., 2005. Experimental design to optimize the
617 degradation of the synthetic dye Orange II using Fenton's reagent. *Catal. Today* 107-108, 68-
618 76.
619
- 620 Ramirez, J.H., Duarte, F.M., Martins, F.G., Costa, C.A., Madeira, L.M., 2009. Modelling of
621 the synthetic dye Orange II degradation using Fenton's reagent: from batch to continuous
622 reactor operation. *Chem. Eng. J.* 148, 394-404.
623
- 624 Ré, J.L., De Méo, M.P., Laget, M., Guiraud, H., Castegnaro, M., Vanelle, P., Duménil, G.,
625 1997. Evaluation of the genotoxic activity of metronidazole and dimetriaizole in human
626 lymphocytes by the comet assay. *Mutat. Res. Fund. Mol. M.* 375, 147-155.
627
- 628 Rivera-Utrilla, J., Prados-Joya, G., Sánchez-Polo, M., Ferro-García, M.A., Bautista-Toledo, I.,
629 2009. Removal nitroimidazole antibiotics from aqueous solution by adsorption/bioadsorption
630 on activated carbon. *J. Hazard. Mater.* 170, 298-305.
631
- 632 Saïdi, I., Soutrel, I., Floner, D., Fourcade, F., N., B., Amrane, A., Geneste, F., 2014. Indirect
633 electroreduction as pretreatment to enhance biodegradability of metronidazole. *J. Hazard.*
634 *Mater.* 278, 172-179.
635
- 636 Sánchez-Polo, M., Rivera-Utrilla, J., Prados-Joya, G., Ferro-García, M.A., Bautista-Toledo, I.,
637 2008. Removal of pharmaceutical compounds, nitroimidazoles, from waters by using the
638 ozone/carbon system. *Water Res.* 42, 4163-4171.
639
- 640 Scott, J.P., Ollis, D.F., 1995. Integration of chemical and biological processes for water
641 treatment: review and recommendations. *Environmental Progress* 14, 88-103.
642
- 643 Shemer, H., Kunukcu, Y.K., Linden, K.G., 2006. Degradation of the pharmaceutical
644 metronidazole via UV Fenton and photo-Fenton processes. *Chemosphere* 63, 293-276.
645

- 646 Spérandio, M., Paul, E., 2000. Estimation of wastewater biodegradable COD fractions by
647 combining respirometric experiments in various S_0/X_0 ratios. *Water Res.* 34, 1233-1246.
- 648 Stasinakis, A.S., 2008. Use of selected advanced oxidation processes (AOPs) for wastewater
649 treatment - a mini review. *Glob. Nest J.* 10, 376-385.
- 650
- 651 Sun, S.P., Li, C.J., Sun, J.H., Shib, S.H., Fand, M.H., Zhoua, Q., 2009. Decoloration of an azo
652 dye Orange G in aqueous solution by Fenton oxidation process: effect of system parameters
653 and kinetic study. *J. Hazard. Mater.* 161, 1052-1057.
- 654
- 655 Tally, F.P., Sullivan, C.E., 1981. Metronidazole in vitro activity, pharmacology and efficacy
656 in anaerobic bacterial infections. *Pharmacotherapy* 1, 28-38.
- 657
- 658 Trujillo, D., Font, X., Sánchez, A., 2006. Use of Fenton reaction for the treatment of leachate
659 from composting of different wastes. *J. Hazard. Mater.* 138, 201-204.
- 660
- 661 Vulliet, E., Cren-Olivé, C., 2011. Screening of pharmaceuticals and hormones at the regional
662 scale, in surface and in groundwaters intended to human consumption. *Envir. Pollut.* 159,
663 2929-2934.
- 664
- 665 Yahiat, S., Fourcade, F., Brosillon, S., Amrane, A., 2011. Removal of antibiotics by
666 integrated process coupling photocatalysis and biological treatment - Case of tetracycline and
667 tylosin. *Int. Biodeter. Biodegr.* 65, 997-1003.
- 668
- 669 Zhou, L., Zhou, M., Zhang, C., Jiang, Y., Bi, Z., Yang, J., 2013. Electro-Fenton degradation
670 of p-nitrophenol using the anodized graphite felts. *Chem. Eng. J.* 233, 185-192.
- 671
- 672 Zhou, M., Yu, Q., Lei, L., Barton, G., 2007. Electro-Fenton method for the removal of Methyl
673 Red in an efficient electrochemical system. *Sep. Purif. Technol.* 57, 380-387.
- 674
- 675
- 676
- 677
- 678
- 679
- 680
- 681
- 682
- 683
- 684
- 685

686

687 **Figures Legends**

688 **Figure 1: a)** Time-courses of MTZ degradation (with or without tert-butanol) and its
689 mineralization during electrolysis. Experimental conditions: C_0 100 mg L⁻¹, I =0.04 mA cm⁻²,
690 $[Fe^{2+}] = 0.1$ mM, pH = 3, $[Na_2SO_4] = 0.05$ M. **b)** Current-potential curve obtained with a
691 vitreous carbon rotating electrode ($S = 3.2 \cdot 10^{-2}$ cm² and 1500 rpm), $r = 5$ mV s⁻¹, under
692 nitrogen atmosphere and $T = 298$ K, for 100 mg L⁻¹ MTZ (continuous line) at pH 3 in Na₂SO₄
693 0.1 M (dashed line).

694 **Figure 2:** Effect of the applied current density on the MTZ degradation **(a)** and its
695 mineralization **(b)**. Experimental conditions: $C_0 = 100$ mg L⁻¹, $[Fe^{2+}] = 0.1$ mM, pH=3,
696 Na₂SO₄=50 mM, V=250 mL.

697 **Figure 3:** Evolution of MTZ degradation with the electric charge for different current
698 densities **(a)** and effect of the current density on the accumulated H₂O₂ production after 1 hour
699 of electrolysis **(b)**. Experimental conditions: $C_0 = 100$ mg L⁻¹, $[Fe^{2+}] = 0.1$ mM, pH=3,
700 Na₂SO₄=50 mM, V=250 mL.

701 **Figure 4: (a)** Effect of the applied current density on the total iron ions concentration.
702 Experimental conditions: $C_0 = 100$ mg L⁻¹, $[Fe^{2+}] = 0.1$ mM, pH=3, Na₂SO₄=50 mM.
703 **(b)** Regeneration of Fe²⁺ at 0.04 and 0.07 mA cm⁻². Experimental conditions $C_0 = 100$ mg L⁻¹,
704 $[Fe^{3+}] = 0.1$ mM, pH=3, Na₂SO₄=50 mM.

705

706

Table 1 : Apparent kinetic rate constants K_{app} obtained during the EF treatment at various initial MTZ concentrations, Fe (II) concentration, pH and applied current intensity.

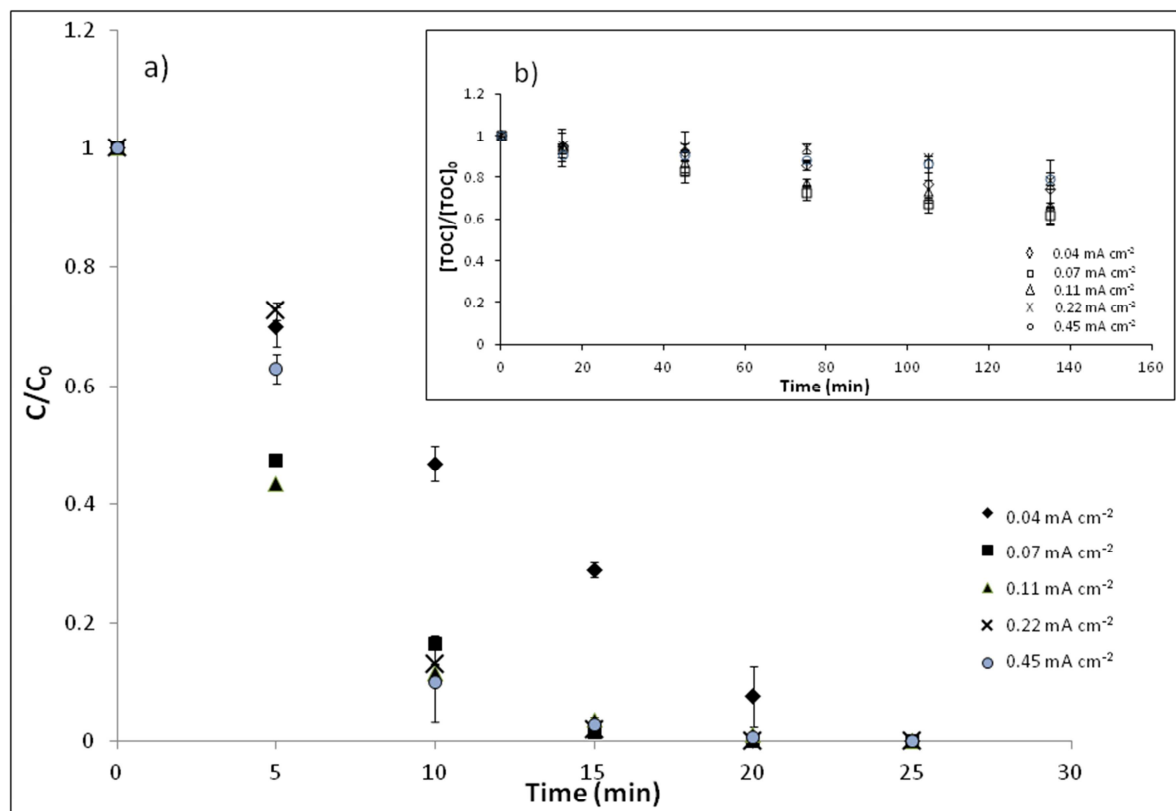
$[MTZ]_{initial}$ ($mg L^{-1}$)	$[Fe^{2+}]$ (mM)	Current density ($mA cm^{-2}$)	pH	kapp (min^{-1})
100	0.10	0.07	3	0.24
200	0.10	0.07	3	0.06
300	0.10	0.07	3	0.04
500	0.10	0.07	3	0.04
100	0.10	0.04	3	0.08
100	0.10	0.11	3	0.22
100	0.10	0.22	3	0.23
100	0.10	0.45	3	0.23
100	0.05	0.07	3	0.15
100	0.5	0.07	3	0.19
100	1.00	0.07	3	0.14
100	0.10	0.07	2	0.18
100	0.10	0.07	5	0.08
100	0.10	0.07	7	0.08
100	0.10	0.07	9	0.08

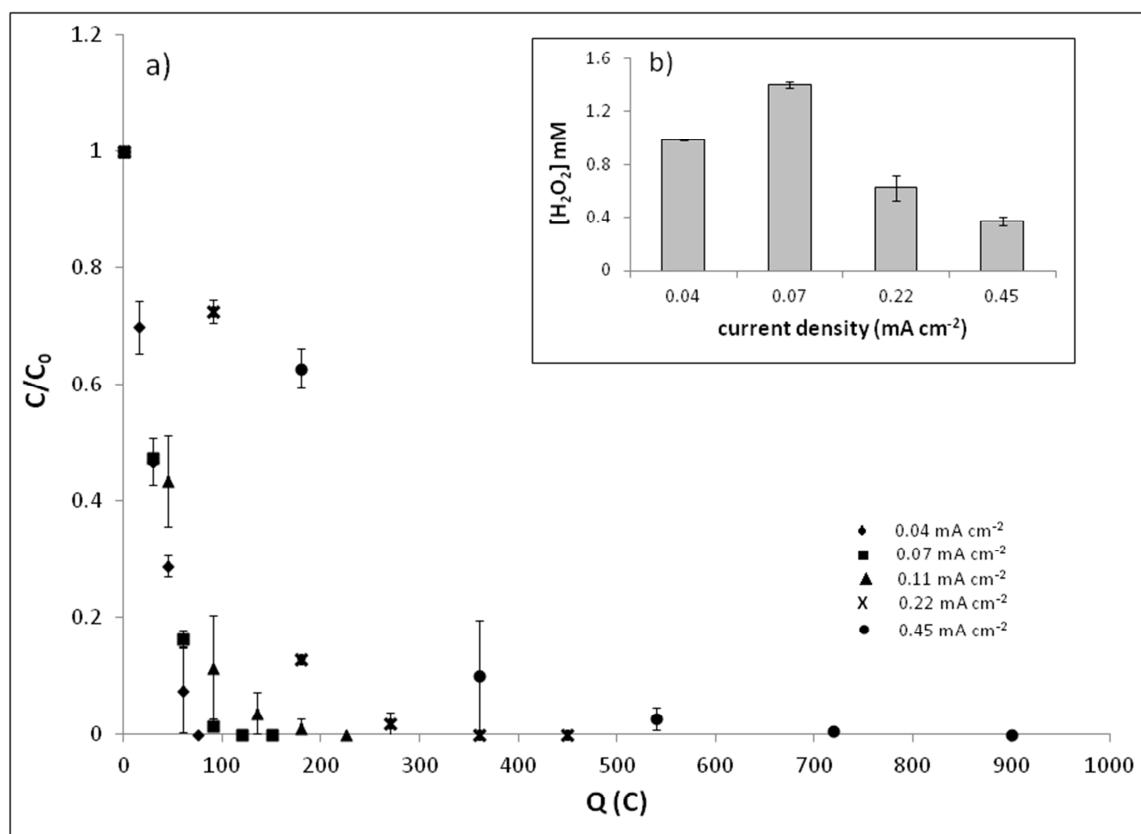
Table2 : Accumulated hydroxyl radicals production obtained during electro-Fenton treatment at various ferrous ion concentrations and various pH

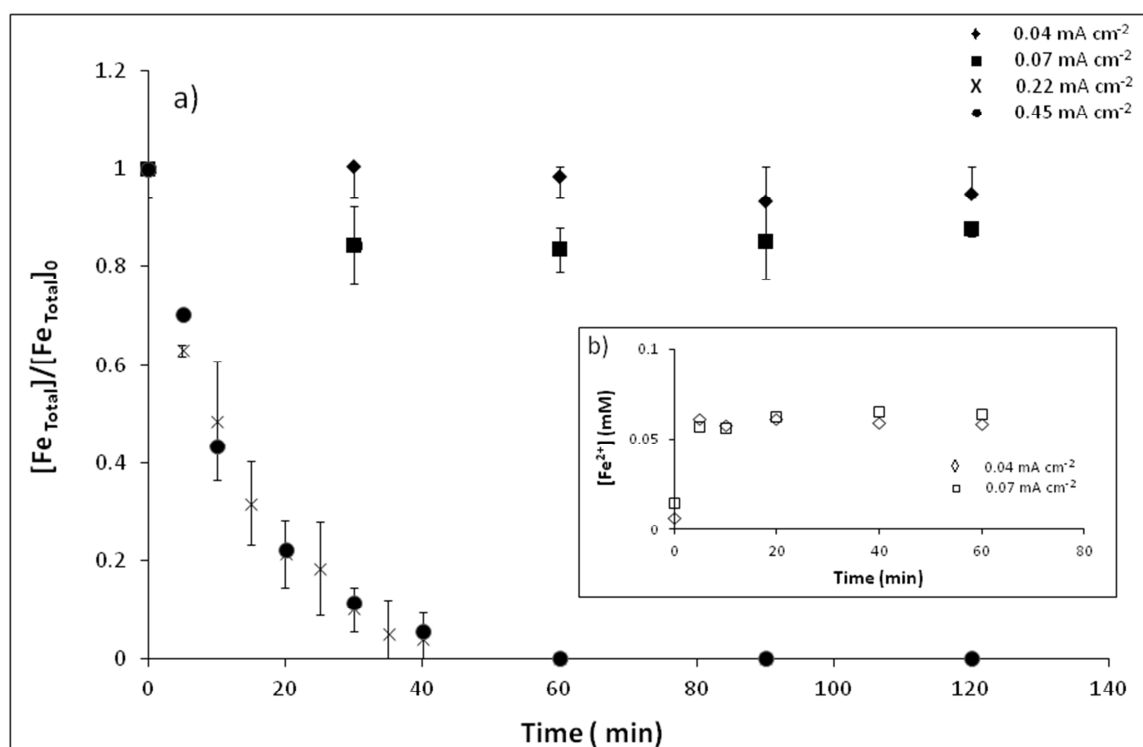
$[MTZ]_{initial}$ ($mg L^{-1}$)	$[Fe^{2+}]$ (mM)	Current density ($mA cm^{-2}$)	pH	$[^{\bullet}OH]$ (mM)
100	0.05	0.07	3	1.52 ± 0.03
100	0.1	0.07	3	2.28 ± 0.01
100	0.5	0.07	3	2.20 ± 0.03
100	1.00	0.07	3	1.56 ± 0.02
100	0.10	0.07	2	1.95 ± 0.09
100	0.10	0.07	5	0.33 ± 0.02
100	0.10	0.07	7	0.29 ± 0.04
100	0.10	0.07	9	0.21 ± 0.02

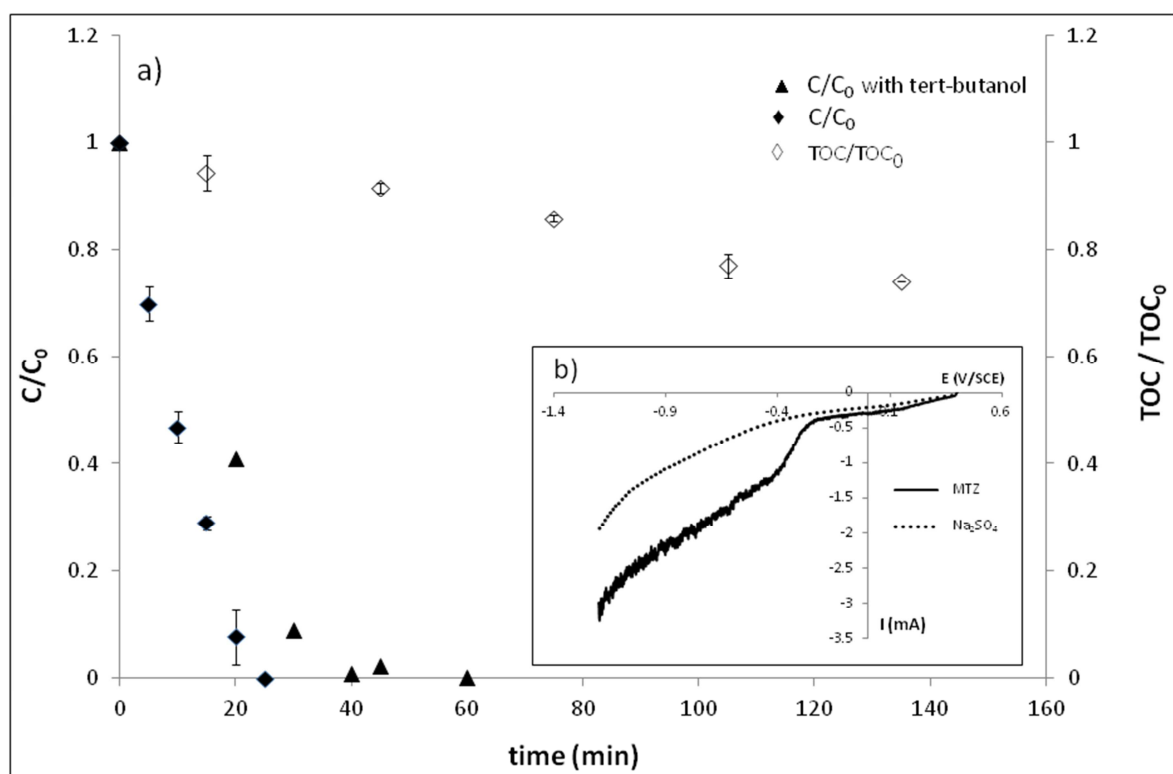
Table 3: Biodegradability of by-product of MTZ. Experimental Conditions: $C_0 = 100 \text{ mg L}^{-1}$ $[\text{Fe}^{2+}] = 0.1 \text{ mM}$, $\text{Na}_2\text{SO}_4 = 50 \text{ mM}$, $V = 250 \text{ mL}$, and 0.07 mA cm^{-2} of current density.

Time (min)	BOD₅/COD
0	0.01
30	0.24
60	0.46
90	0.46
120	0.70









Highlights

- MTZ electroreduction involved in its degradation not in its mineralization
- Good regeneration of ferrous ions up to $0.07 \text{ mA}\cdot\text{cm}^{-2}$
- Highest $\cdot\text{OH}$ production for $0.07 \text{ mA}\cdot\text{cm}^{-2}$, pH 3 and 0.1 mM of ferrous ions
- Limit of biodegradability reached for 60 min of electrolysis according to BOD₅ test
- Results from BOD₅ reinforced by respirometric study implemented during 21 days